第19卷第2期 1997年6月 湘潭大学自然科学学报 Natural Science Journal of Xiangtan University Vol. 19 No. 2 Jun. 1997

THERMAL SHOCK WAVE AND SPALL FRACTURE CAUSED BY AN ELECTRON BEAM

Zhou Y C[①] *Duan Z P*[②] *Yang Q B*[①]

(① Department of Physics, Xiangtan University, Xiangtan, 411105

② Institute of Mechanics, Chinese Academy of Sciences, Beijing, 100080)

[Abstract] Thermal shock wave and spall effect of LY-12 aluminum exposed ro a highcurrenr and low-energy electron beam are studied. The mechanism of energy deposition of electrons in the target is very complicated. Many researchers used the Monte-Carlo method to calculate the energy deposition, bur a semi-empirical method is used in this paper. The melting process should be adequately taken into account for the studies of the material dynamic response in the intermediate energy deposition range. The equation-of-srare (EOS) model used is a three-phase EOS which provides a more detailed and thermodynamically complete descriprion of metals in the melting region. We also use the srrain-rate-dependent constitutive model which is more effective than the simple von-Mises elastic-plastic model in studying the spall fracture and the attenuation of the propagaring stress waves. The heat-conduction effect is also considerd. The calculated results are in good agreement with the experimental results.

1 Introduction

It is useful, in the fields of radiation hardening, nuclear electricity generating plants and laser weapons, to study the effects of rapid energy deposition in a variety of high-speed phenomena. Such phenomena include: the deposition of x-ray energy from the detonation of nuclear explosives, the deposition of electrons from electron-beam machines, the deposition of intense laser beam energy, exploding wire phenomena and the explosive compression of magnetic flux. All of these phenomena may be characterized by high energy densities and take place over times of the order of a few nanoseconds to a few hundred nanoseconds. Although the mechanisms of energy deposition of thse phenomena are varied, the deposited energy all causes a shock wave in the target. The tensile stress may appear near the rear free surface due to the reflection of the shock waves. If it is strong enough, the tensile stress may lead the spallation of the farget. The melting process is important for the study of material dynamic response in the intermediate energy deposition range. Application of the simple Mie-Grüneisen EOS model to the intermediate range may be questionable and deserves careful scrutiny. A more complicated three-phase EOS, the so-called GRAY EOS, has been developed by Royce[1] for the treatment of metals in the intermediate range. It offers the advantage of explicit treatment of the melting transition with some degree of sophistication. The strain rate is very high in high speed phenomena and, the strain rate may be up to $10^7 s^{-1}$ in

the energy deposition of intense laser beam[2].

The constitutive equation of a simple von Mises type elastic - plastic model should be replaced with a more sophisticated strain rate dependent model to describe plastic flows. In this paper, a strain rate dependent model[3]is used to study the attenuation of the propagating stress waves and the spall effect. The spall model used is the cumulative damage criterion developed by Tuler and Butcher[4].

2 Theoretical model

The material exposed to a short pulse of electron beam will attempt to thermally expand under the rapid indepth heating. As the heated region expands in response to the thermal pressure, a portion of the hot material as the form of liquid will be blown off from the front of the sample. The phenomena of the melting, vaporization as well as the plasma generation on the surface of the target material in the incident particles - materials interaction are different from that in the mechanical loading. Although dynamic loading conditions are different, shock wave phenomena produced by dynamic loadings are commonly the same in both cases. This strong shock wave may lead the spallation due to the wave reflection from the rear free surface of the targets. To model the thermal shock wave and spall damage one must consider the interaction of incident electrons with materials, the surface melting, the propagationg of stress waves as well as the fracture in solids. One dimensional elastic - plastic hydrodynamic equations in uniaxial strain configurations are expressed as in the following

$$\text{Continuity}: V=\frac{\mathrm{I}}{\rho_0}\frac{\partial R}{\partial r} \tag{1}$$

$$\text{Momentum}: \frac{\partial u}{\partial t}+\frac{\mathrm{I}}{\rho_0}\frac{\partial \sigma}{\partial r}=0 \tag{2}$$

$$\text{Energy}: \frac{\partial E}{\partial t}+\sigma\frac{\partial V}{\partial t}=E_D+VK\frac{\partial^2 T}{\partial r^2} \tag{3}$$

$$\text{Constitutive model}: \sigma=P+\frac{4}{3}\tau=P+\frac{4}{3}\mu(\varepsilon-\frac{3}{2}\varepsilon_P) \tag{4}$$

$$\text{EOS}: P=\textcircled{H}(E,V),\quad T=\Phi(E,V) \tag{5}$$

where R and r are, respectively, Eulerian and Lagranian coordinates, t time, and the eleven variables, that is, ρ_0 the initial mass density, V specific volume, σ total stress (taken positive in compression), ε_p plastic strain, E specific energy, E_D deposited specific energy rate, P pressure and T temperature which both are the function of E and V, t shear stress, μ shear modulus, K thermal conductivity. The particle velocity u and total strain ε are, respectively, defined as:

$$u=\frac{\partial R}{\partial t},\qquad \varepsilon=\ln(\rho/\rho_0) \tag{6}$$

where $\rho=V^{-1}$ is the mass density. The artificial viscosity q is given as:

$$q=\begin{cases}a_1 c\dfrac{\Delta t_1}{r}\left|\dfrac{\partial r}{\partial t}\right|+a_2^2\left(\dfrac{\Delta r_1}{V}\right)^2\left(\dfrac{\partial u}{\partial r}\right)^2, & \dfrac{\partial u}{\partial r}<0\\ 0\ , & \dfrac{\partial u}{\partial r}\geqslant 0\end{cases} \tag{7}$$

where a_1 and a_2 are viscosity coefficient, c is the velocity of sound, Δt_1 and Δr_1 are, respectively, time and space increment in the calculation.

The cumulative damage criterion is based on the consideration of a function Fand defined as[4]:

$$F(\sigma,t)=\int_0^{\Delta t}(\sigma_0-\sigma)^{\beta}\mathrm{d}t,\quad \text{for } \sigma\leqslant\sigma_0 \tag{8}$$

where σ_0 is a constant tensile stress at which the cumulative damage calculation is initiated, β is a coefficient, and Δt respesents the width of the tensile pulse at the stress level $\sigma_0-\sigma$. The cumulative damage criterion states that spall will take place in the material at the points where the function F equals or exceeds a critical f. For incipient spall, the maximum value of the function F equals f.

3 Energy Deposition

When an electron beam radiates on a target, any or all of the following collision processes may take place – not to mention nuclear reactions and other strong interactions – and in their course bring about energy diminution and deflection of the incident particles'motion: (1) inelastic collisions with atomic electrons, (2) inelastic collisions with nuclei, (3) elastic collisions with atomic electrons, (4) elastic collisions with nuclei.

Inelastic collisions are the primary mechanism by which beta particles (incident electrons) lose the energy in matter. Usually inelastic collisions with atomic electrons result in excitation or freeing of the atomic electrons. The energy losses caused by this collision processes are called ionizable losses. Inelastic collisions with nuclei, on the other hand, result in deflections of the incident beta particles. During the deflection, a quantum of electromagnetic radiation (bremsstrahlung) may be emitted. The kinetic energy of the beta particle is reduced by an amount equal to the bremsstrahlung energy. The energy losses caused by this collision processes are called radiative losses. Ionizable losses dominate at low beta energy and radiative losses dominate at high beta energy.

In elastic collisions with electrons and nuclei, the incident beta particle is deflected but it does not radiate energy. During an elastic collision with a nucleus, the beta particle only loses enough energy to conserve momentum between the colliding particles. For an elastic beta – electron collision, energy and momentum are conserved and generally not enough energy is transferred to excite the struck electron.

The type of interaction which occurs during each collision is a matter of chance. The probability of each type of encounter can be obtained from scattering theory. So many inves-

tigators used the Monte - Carlo method to study the interaction of an electron beam with matter. In this paper, to avoid the complicated numerical calculation we present a simple model for the energy deposihion of pulsed electron beams in materials.

Suppose that an electron beam which has $N_0(t)$ electrons per unit area and per unit time impinges normally on a target. The incident electron beam is multienergetic and consis of m kinds of energy. ε_{0j} is the fraction of the energy E_{0j}. The penetration depth in the incident direction is defined as the effective mean range R_{0j}. For the low - energy electron beam and low atomic number Z target, the following empirical expression for the effective mean range R_0j (in g/cm^2)as a function of kinetic energy E_{0j}(in Mev) was proposed by Rudie[5]:

$$R_{0j} = G_1 E_{0j}^{G_2 - G_3 \ln R_{0j}} \tag{9}$$

The penetration depth in the incident direction of eletrons away from the incident surface r (cm), where kinetic energy is E_j, is defined as remanet effective mean range R_j(in g/cm^2):

$$R_j = G_1 E_j^{G_2 - G_3 \ln E_j} \tag{10}$$

where G_1, G_2 and G_3 are material constants, for aluminum alloy $G_1 = 0.5493$, $G_2 = 1.216$, $G_3 = 0.11$.

From (9) and (10), the kinetic energy E_j away from the surface r is expressed as follows:

$$E_j = \exp\left\{\frac{0.5}{G_3}\left[G_2 - \left(G_2^2 - 4G_3 \ln \frac{R_{0j} - \rho r}{G_1}\right)^{1/2}\right]\right\} \tag{11}$$

Subba[6] gave an empirical expression for the transmission in the incident direction of the electrons from many theoretical and experimental data as in the following.

$$T_j = \frac{1 + \exp(-nn_0)}{1 + \exp[n(\rho r - n_0 R_{0j})/R_{0j}]} \tag{12}$$

where $n = 9.2Z^{-0.2} + 16Z^{-2.2}$, $n_0 = 0.63(Z/A) + 0.27$, A is atomic weight (in g/mole).

When the dynamic coupling of energy deposition and the propagating stress wave is considered, the deposited specific energy rate E_D(in Mev/g. s) may be calculated from Eqns(11) and (12) through.

$$E_D = -\sum_{j=1}^{m} \varepsilon_{0j} N_0(t) \frac{\mathrm{d}}{\mathrm{d}r}\left(\frac{T_j E_j}{\rho}\right) \tag{13}$$

Which will play an important role in the study of the beam induced stess wave propagation, as issued in the Section 2 and section 6. The readers who are assumed not familiar with the approximate expressions used for the deposited energy from an electron beam are referred to Ref[5].

4 Constitutive Model

When the propagation and attenuation of thin stress pluses are of great concern, the constitutive model is important. As is generally known, the simple elastic plastic consitutive model cannot account for increases in the flow stress due to strain hardening and strain rate

effects, or changes in the nature of strain hardening or reverse loading from a prestrained state (Bauschinger effect). It has been apparent for some time that many metals exhibit to some degree dynamic response features which the simple elastic plastic model does not account for. Moreover, experimental evidence indicates that some of the more complex effects not exhibited by the simple elastic plastic model may have significient influence on the calculation of thin pulse propagation and damage thresholds in metals.

In this paper, the constitutive model proposed by Read[3] is used. In the constitutive model, the total strain ε is decomposed into elastic and plastic components. The elastic component is obtained from Hook's law, and the plastic stain is obtained from the theory of dislocation dynamics in which the plastic strain rate is related to the mobile dislocation density and the average dislocation velocity. The model describes a spectrum of mechanical response ranging from quasistatic behavior, through the thermally activated intermediate strain rate region, and upto the high strain rate region, where phonon viscosity and sonic relativistic effects control the plastic flow process. Upon reverse loading from a prestrained state, the constitutive model exhibits a rate dependent Bauschinger effect.

When we do not distinguish between dislocation types (slip and twinning deformation) in the one dimensional configurations considered herein, the plastic strain rate component $\dot{\varepsilon}_p$ in the direction of uniaxial strain is given as:

$$\dot{\varepsilon}_p = \frac{4}{3} b N_m V_D \tag{14}$$

where b is Burgers vector, N_m is density of the mobile dislocations, V_D is mean velocity of the mobile dislocations.

The applied shear stress τ may be decomposed into a thermal component τ_T which depends on the temperature T and the plastic strain rate $\dot{\varepsilon}_p$, an athermal component τ_A which depends on the plastic strain and reflects strain hardening and the Bauschinger effect, and a viscous drag stress component τ_D which is rate dependent and reflects the influence of viscous drag. Thus the applied shear stress τ is given as:

$$\tau = \tau_T + \tau_A + \tau_D \tag{15}$$

For most metals in which thermal activation does not play an important role at a given temperature, the thermal component τ_T may be neglected. This means that the thermal degradation is neglected. When this is the case, the glide velocity u_g is equal to the mean velocity of the mobile dislocations. From the relativity theory[3] we have:

$$V_D = \sqrt{1 - V_D^2/C_t^2}\,\psi \tag{16}$$

where C_t is the elastic shear wave velocity, ψ is a nonlinear function of τ_D:

$$\psi = \alpha_1 \tau_D + \alpha_2 \tau_D^2 \tag{17}$$

where α_1 and α_2 denote constants evaluated from experimental data. From (14) to (17), we have:

$$\dot{\varepsilon}_p = \frac{4}{3}\frac{N_m b\psi}{\sqrt{1+\psi^2/C_s^2}} \tag{18}$$

$$\psi = \alpha_1(\tau-\tau_A)+\alpha_2(\tau-\tau_A)^2 \tag{19}$$

When strain hardening and the Bauschinger effect are considered, the athermal τ_A is given as:

$$\tau_A = \alpha\tau_0[1+A\varepsilon_{pc}+|-\varepsilon_p|^{\Delta}]^{1/2}[1-c'\exp(-\delta\sqrt{|\varepsilon_{pc}-\varepsilon_p|})] \tag{20}$$

where τ_0 is the initial yield stress, A, Δ and δ are constants determined from experimental data, α has the value of 1 or -1, and c' has the value of 1 or 0, depending on where there is initial loading, reverse loading or subsequent loading. Furthermore, ε_{pc} denotes the maximum value of ε_p obtained during the previous phase. Finally, ε_{pc} represents the accumulated generalized plastic strain.

The mobile dislocation density N_m depends most strongly on the plastic strain ε_p:

$$N_m = \begin{cases} N_{m\infty}+(N_{m0}-N_{m\infty}+M\varepsilon_p^2)\exp(-A_1\varepsilon_p), & \text{for initial loading} \\ N'_{m\infty}+(N_m^*-N'_{m\infty})\exp(-A_2\bar{\varepsilon}_p^2), & \text{for reverse loading} \end{cases} \tag{21}$$

where N_{m0} denotes the initial mobile dislocation density, $N_{m\infty}$ is the asymptotic value of N_m for continued initial loading, M represents a dislocation multiplication coefficient, A_1 and A_2 are annihilation coefficients, $N'_{m\infty}$ is the asymptotic value of N_m during continued reverse loading, $\bar{\varepsilon}_p$ is defined as:

$$\bar{\varepsilon}_p = \varepsilon_p^* - \varepsilon_p \tag{22}$$

where $\bar{\varepsilon}_p^*$ is the value of ε_p at the end of the initial loading process and N_m^* is the value of N_m at ε_p^*.

An inspection of equation (18) reveals that it is of the general form:

$$\dot{\varepsilon}_p = g(\varepsilon_p, \tau) \tag{23}$$

where the function g depends in a nonlinear manner on both ε_p and τ. So the shear stress can be obtained from (4) and (23), however, at the very onset of melting, it is assumed to be zero.

5 Three-Phase EOS

The-simple Mie-Grüneisen(M-G) equation of state is employed to describe the thermodynamic states of the solid and liquid phase, and a join to some sort of gas-law equation is forced for expanded volume states at high temperatures. This procedure proves adequate in many cases of interest. But for simple M-G EOS, no distinction is normally made between the solid and liquid states, nor are the details of the melting transition considered.

In this paper, the deposited energy is in the state that causes the surface material melting. Therefore, the internediate region(i.e. for pressures and temperatures near the melting transition) is important. For solids heated to high temperatures, i.e., above the onset of

melting, an accurate thermodynamic description is more complicated. In particular, the existense of multiple phases must be treated as well as the effects of the melting (and boiling) transition. The GRAY EOS is adequate to describe the intermediate region.

In the GRAY EOS, the solid - liquid region is described by scaling law equation of state for metals developed by Grover[7] who assumed that: (1) entropy of melting is a constant and independent of the material or the pressure; (2) the temparature dependence of the specific heat in the liquid is a universal curve and scaled on the melting temperature; (3) the melting temperature T_m is taken as a function of volume by integrating a modified Lindemann law. The effect of the nondegeneracy of the conduction electrons at nonzero temperature is added in a free - electron approximation. The scaling - law EOS also includes a Grüneisen description of the solid.

The specific thermal energy $E_T(T,V)$ and the thermal pressure $P_T(T,V)$ are described by a scaling - law EOS as follows:

solid, i.e. $T \leqslant T_m(V) - \delta T(V)$

$$E_T(T,V) = 3R'T + \frac{1}{2}G'T^2 = E_T^s(T,V) \tag{24}$$

$$VP_T(T,V) = 3\gamma_s(V)R'T + \frac{1}{2}\gamma_e G'T^2 = VP_T^s(T,V) \tag{25}$$

melt, i.e. $T_m(V) - \delta T(V) \leqslant T \leqslant T_m(V) + \delta T(V)$

$$E_T(T,V) = E_T^s(T,V) + \upsilon[T - \upsilon\delta T(V)](\Delta s' - \alpha') \tag{26}$$

$$VP_T(T,V) = VP_T^s(T,V) + \lambda(V)\upsilon T_m(V)(\Delta s' - \alpha') \tag{27}$$

liquid, i.e. $T_m(V) + \delta T(V) \leqslant T \leqslant T_C(V)$

$$E_T(T,V) = E_T^s(T,V) + T_m(V)\left\{\Delta s' - \frac{\alpha'}{2}\left[1 + \frac{T^2}{T_m^2(V)}\right]\right\} \tag{28}$$

$$VP_T(T,V) = VP_T^s(T,V) + \lambda(V)T_m(V)\left\{\Delta s' - \frac{\alpha'}{2}\left[1 + \frac{T^2}{T_m^2(V)}\right]\right\} \tag{29}$$

hot liquid, i.e. $T \geqslant T_C(V)$

$$E_T(T,V) = E_T^s(T,V) + T_m(V)\left\{\Delta s' + \frac{\alpha'}{2}\left[\left(\frac{3R'}{2\alpha'}\right)^2 - 1\right]\right\} \tag{30}$$

$$VP_T^s(T,V) = VP_T^s(T,V) + \lambda(V)T_m(V)\left\{\Delta s' + \frac{\alpha'}{2}\left[\left(\frac{3R'}{2\alpha'}\right)^2 - 1\right]\right\} - \frac{3}{2}\lambda(V)R'T \tag{31}$$

In these expressions, $E_T^s(T,V)$ and $P_T^s(T,V)$ are the specific thermal energy and thermal pressure at a temperature and specific volume T and $V = \rho^{-1}$, described by a Grüneisen - type EOS, or to the extrapolation of the Grüneisen solid EOS to high temperature, $\delta T(V)$ is temperature change on melting at constant volume, $R' = R/A$, R is the gas constant, G' is the electronic energy coefficient, $\gamma_s(V)$ is the volume - dependent Grüneisen gamma for the solid, γe is the electronic gamma, υ is a progress variable describing melting, $\lambda(V)$ is the slope of the melting line, $\Delta s'$ is the entropy of melting, α' is a parameter describing the rate of decrease of the specific heat in the liquid, $T_C(V)$ is the temperature at which the hot liquid begins to behave thermally like an ideal gas. At a particular specific volume, melting is as-

sumed to start at a temperature $T_m(V)-\delta T(V)$ for the solids, and to be complete at a temperature $T_m(V)+\delta T(V)$ for the liquids.

In GRAY EOS, it is assumed that the liquid – vapor region may be described by a hard – sphere model perturbed by a van der Waals attraction. The EOS is developed by Yong and Alder[8]. Their van der Waals model used an analytical representation of the classical hard – sphere EOS with a van der Waals attractive term added. The two parameters in the theory can be evaluated from the cohesive energy and the density of the liquid near the melting point. The pressure and specific energy $P(T,V)$ and $E(T,V)$ are described by the following equations:

$$P(T,V)=\frac{R'T(1+Y+Y^2-Y^3)}{V(1-Y)^3}-\frac{\alpha'_Y}{V^2} \tag{32}$$

$$E(T,V)=\frac{3}{2}R'T-\frac{\alpha'_Y}{V} \tag{33}$$

where $\alpha'_Y=\alpha_Y/A^2$, α_Y is the Young – Alder – van der Waals coefficient. The variable Y is a scaled density, $Y=V_b/V$, $V_b=0.45V_L$, where V_L is the specific volume of the liquid near the melting point.

The complete EOS is developed by analytically joining the Grover scaling law and the Young – Alder models at a volume in the range 1.3 to 1.5 times normal volume. This is accomplished by adding correction terms to the Young – Alder EOS employed on the low – density side of the join volume. These correstion terms make the EOS continuous at the join volume by slightly modifying the Young – Alder EOS in that vincity. They become insignificant at volumes welll away from the join volume, leaving the Young – Alder EOS unaffected. All of this is done in a thermodynamically consistent manner.

The equation of state is laid out in $P=\Phi(E,V)$ and $T=\Phi(E,V)$ forms for use in numerical hydrodynamics calculation. For a detailed description of the GRAY EOS, the reader is referred to the original literature[1].

6 Results

In this section we present the calculated results of energy deposition, specific energy by the end of electron beam radiating, attenuation of stress wave peak value, thermal shock wave shape, position – time plot and spall effects. We also compare some calculated results with the experimental results. As metioned above, the term of the deposited energy in (3) is calculated from Section 3, the constitutive model and EOS are, respectively, calculated from Section 4 and 5.

The composition of LY – 12 aluminum is very similar to 2024 aluminum. Therefore, the parameters of 2024 aluminum for three – phase GRAY EOS[1] are selected as those of the target. Whereas the parameters of the strain rate dependent constitutive model[3] and the cumulative damage criterion[9] of 6061 – T6 aluminum are selected as those of the target LY – 12 a-

luminum, respectively. The thermal conductivity is 1.2(W/cm. K) for the solid LY-12 aluminum. However, for the liquid region the thermal conductivity is selected to be 0.8(W/cm. K) from the reference[10].

The experiments were carried out with 1MV electron beam machine[11]. The diode voltage is 0.67 MV and current intensity is 16KA and the cathode-to-anote gap in the field emission tube is 12mm. The vacuum is 6.7×10^{-3}Pa. This mode of operation produced a beam with a relatively constant energy distribution (the mean energy of the electrons is 0.267Mev), which is multienergetic and Fig. 1 illustrates its energy spectrum, yet with a fluence 32cal/cm^2, the resulting beam is a stable pulse of electrons having a full width at half-maxium of 25ns.

Although the measured diode emission current is not accurate, it is very similar to sinusodial shape from the measurements. The current $I(t)$ incident on the target is assumed to have the same time dependence and current intensity as the diode emission current. Therefore, we have $I(t)=I_0\sin(\omega t)$, where $I_0=16KA$ is the peak current intensity, $\omega=2\pi/75\text{ns}^{-1}$ and the pulse duration is 37.5ns.

The target samples (i.e., the anode) are 30mm-diam disks of LY-12 aluminum. The beam spots are 10mm in diameter. The rear surface is closely struck on a quartz crystal to measure the normal velocity histories of the surface.

The disks with five different thickness, 1.2, 1,5, 2.0, 2.8 and 4.0mm are used in order to observe the amplitude of stress ware in different shot and to compare them with theoretical predictions.

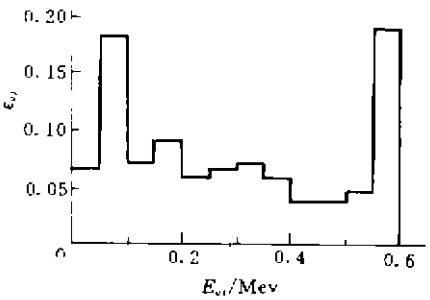

Fig1 Energy of an electron beam spectrum

when a monoenergetic electron beam with 1 Mev energy impinges normally on aluminum target, the specific energy Q (Mev/g·cm^2) deposited on per unit area is illustrated in Fig. 2. To check the simple model of energy deposition (13), we also compared the calculated results of the energy deposition with the experimental data given in Ref[5]. As seen in Fig. 2, the magnitudes of the calculated energy deposition agree approximatelly with the measured values.

In Fig. 3, the specific energy by the end of electron beam radiating is illustrated. It can be seen that the deposited energy just exceeds the energy necessary to melt the target surface materials. So the material, especially the heated surface region, is in the intemediate region (i.e., for pressures and temperatures near the melting transition).

In Fig. 4, the attenuation of stress wave peak value is illustrated. The attenuation of stress wave peak value is very strong near the incident surface. It can be seen that the calculated values are basically consitent with the experimental values. In Fig. 5 the thermal shock wave shape shows that the shock wave becomes wider and wider as the propagating stress

wave deepens into the solid region. This phenomenon is natural.

We also give the position – time plot in Fig. 6. Region I and Ⅰ in this plot represent the hot liquid region and liquid, respectively. They are blown off as a result of the thermal pressure . Region Ⅱ and Ⅳ represent the melt and solid region, respectively. As a result of the heat – conduction effect and the propagating of the thermal shock wave, the melt region will vanish. The phenomenon may also regarded as the resolidfication of the melting region. In the experiment, we have obviously observed the "blown off" materitals and the resolidified materials. Their thickness is basically cosnistent with the theoretical values. From the position – time plot, we may see that the incident surface regions are very complicated.

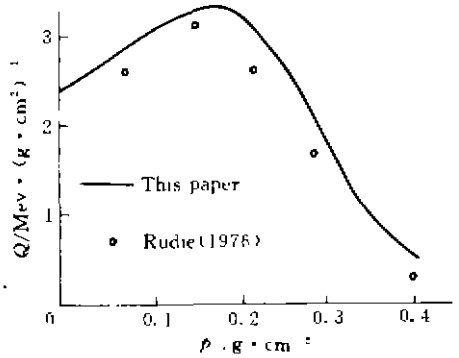

Fig 2 Energy deposition for 1.0 m_{e_0} electron beam in the aluminum target

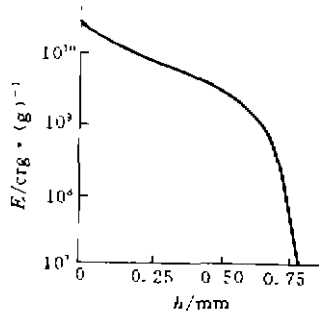

Fig 3 Specific energy by the end of electron beam radiating

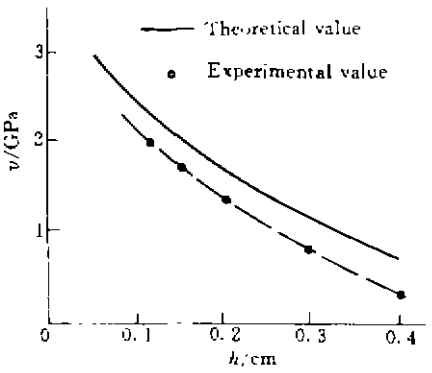

Fig 4 Attenuation of stress wave peak value

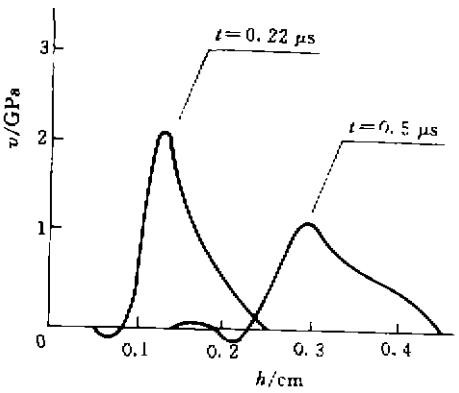

Fig 5 Thermal shokc wave shape

Table 1 gives the calculated and experimental results of spall effects near the rear free surface of the target samples. The spalls become thicker and thicker as the target thickness increases by degrees. This is due to the fact that the shock wave is very narrow and the tensile stress is much greater than the fauilure intensity σ_0 when the target is thin. Therefore, the cumulative damage time Δt is very short and so short that the spall becomes thin. Where-

as the target is thick the shock wave width increases and the tensile stress is just a little greater than the failure intensity σ_0 and, therefore, the cumulative damage time Δt is very long and so long that the spall becomes thick. However, the spall effect can't take place as the target thickness increases to a certain degree. This is due to the fact that the tensile stress causes the function F of the cumulative damage criterion less than the critical f under these circumstances. The calculated and experimental results all show that spall takes place only once.

7 Conclusions

In this paper, we propose a semi - empirical formula for studying the energy deposition of an electron beam in the target. The results of a theoretical study of the dynamic response of LY - 12 aluminum exposed to a high - fluence low - energy pulsed electron beam are presented and compared with some experimental results. The consistancy of the calculated results with the experimental results shows the importance of EOS. Because of the existence of multiple phases, the state, especially near the incident surface, is very complicated. When fluences become higher and hence higher strain rates and plasma may come into existance, in thiscase, the multiphase EOS and the strain rate dependent constitutive mode become more important.

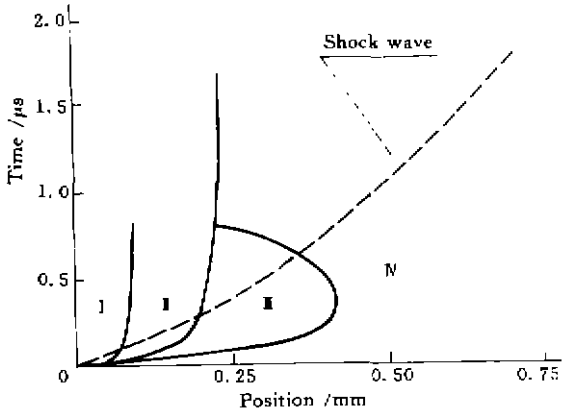

Fig 6 Position - time plot(I - hot liquid, II —liquid, III —melt, IV — solid)

Moreover, there are microvoids in the materials and the microvoids will change because of void diffusion, void nucleation and void growth. The temperature, strain, strain - rate, incident particles (electron beam, laser beam, x - ray)all effect the change of microvoids. Some constitutive models for a solid with microvoids as a means for modeling deformation at high strain rates coupled with material damage have been proposed by krajcinovic[12], Perzyna[13], ad Nemes et al[14] and zhou et al[15].

Table 1 Spall thickness δ of LY - 12 aluminum targets

Target thickness(mm)	1.2	1.5	2.0	2.8	4.0
δ theore. (mm)	0.34	0.35	0.39	0.43	0
δ exper. (mm)	0.41	0.41	0.42	0.46	0.48

References

1 Royce E B. GRAY, A Three - Phase Equation of State for metals. Lawrence Livermore Laboratory, Report UCRL - 51121,1971

2 Eliezer S, Gilath I. Laser - Induced Spall in Metals: Experiment and Simulation. J Appl Phys, 1990,67:715～724.

3 Resd H E, Triplett T R, Cecil R A. Dislocation Dynamics and the Formulation of Constitutive Equations for Rate - Dependent Plastic Flow in metals. Systems Science and Software, Report DASA - 2638, 1970

4 Tuler F R, Butcher B. A Criterion for the Time Dependence of Dynamic fracture. Int J Fract Mech, 1968, 4: 431～437

5 Rudie J N. Principles and Techniques of Radiation Hardening. California, Western Periodicals Company, 1976

6 Subba Rao B N. S Simple Formula for the Transmission and Absorption of Monoenergetic Electrons. Nucl Instr Mech, 1966,44: 155～156.

7 Grover R. Liquid metal Equation of State Based on Scaling. J Chem Phys,1977, 55:3435～3431.

8 Young D A, Alder B J. Critical Point of Metal From the van der Waals Model. Phys Rev A, 1971(3):374～371.

9 Larson A R. Calculation of Laser Induced Spall in Aluminum Targets. Los Alamos laboratory Report, LA - 5619 - MS, 1974

10 Von Allmen M, Laser - Beam Interactions with Materials. Berlin, Springer - Verlag, 1987: 60～61

11 *Peng C X. Experimental Studies of the Thermal Shock Wave Produced in Aluminum Alloy Bombarded by Electron* Beam. Explosion and Shock Waves(in Chinese), 1987(7): 250～256.

12 Krajcinovic D. Constitutive Equations for Damaging materials. ASME J Appl Mech, 1983, 50:355～360.

13 Perzyna P. Internal State Varible Description of Dynamic Fracture of Ductile Solids. Int J Solids Structures, 1986,22: 797～818

14 Nemes J A, Eftis J, Randles P W. Viscoplastic Constitutive Modeling of High Strain - Rate Deformation, Material Damage, and Spall Fracture. ASME J Appl Mech, 1990,57:282～291.

15 Zhou Y C, Duan Z P, Yan X H. Thermal Stress wave and Spallation Induced by An Electron Beam. Int J Impact Engng, 1997

(27)
117-128

电子束引起的热击波和层裂破坏效应*

周益春[1)] 段祝平[2)] 杨奇斌[1)]

0347.51

【摘要】 本文对强流低能相对论电子束引起 LT - 12 铝产生的热击波和层裂进行了分析. 电子束在靶材中的能量沉积是非常复杂的,通常都用 Monte - Carlo 数值模拟的方法来计算能量沉积,本文发展了一种新的半经验解析方法. 在研究由电子束引起材料的动态响应时,对于靶材表面的熔化过程要进行适当考虑,本文使用了 GRAY 三相状态方程,详细考虑了这种复杂的溶化过程. 同时在研究层裂破坏效应及应力波的衰减规律时,放弃了通常的 von - Mises 流体弹塑性模型,而使用了应变率相关的本构模型. 计算结果和实验结果比较一致.

主题词 电子束;热击波;层裂
分类号 TN24

数值模拟
能量沉积

* 国家 863 激光技术领域,国家自然科学基金,湖南省教委资助项目
作者单位:1)湘潭大学物理系,湘潭,411105;2)中国科学院力学研究所,北京,100080
收稿日期:1996 - 03 - 22